Knoxville, Tennessee, USA, April 15-20, 2012, on CD-ROM, American Nuclear Society, LaGrange Park, IL (2012)

SENSITIVITY ANALYSIS OF MONJU USING ERANOS WITH JENDL-4.0

P. TAMAGNO
Institut National des Sciences et Techniques Nucléaires
INSTN - Point courrier n° 35
Centre CEA de Saclay
F-91191 Gif-sur-Yvette Cedex FRANCE
pierre.tamagno@mines-saint-etienne.org

W. F. G. Van ROOIJEN, T. TAKEDA
Research Institute of Nuclear Engineering
University of Fukui
T914-0055 Fukui-ken, Tsuruga-shi
Kanawa-cho 1-2-4 JAPAN
rooijen@u-fukui.ac.jp ; t_takeda@u-fukui.ac.jp

M. KONOMURA
Japan Atomic Energy Agency
FBR Plant Engineering Center
919-1279 Fukui-ken, Tsuruga-shi
Shiraki 1 JAPAN
konomura.mamoru@jaea.go.jp

ABSTRACT

This paper deals with sensitivity analysis using JENDL-4.0 nuclear data applied to the Monju reactor. In 2010 the Japan Atomic Energy Agency – JAEA – released a new set of nuclear data: JENDL-4.0. This new evaluation is expected to contain improved data on actinides and covariance matrices. Covariance matrices are a key point in quantification of uncertainties due to basic nuclear data. For sensitivity analysis, the well-established ERANOS [1] code was chosen because of its integrated modules that allow users to perform a sensitivity analysis of complex reactor geometries. A JENDL-4.0 cross-section library is not available for ERANOS. Therefore a cross-section library had to be made from the original nuclear data set, available as ENDF formatted files. This is achieved by using the following codes: NJOY, CALENDF, MERGE and GECCO in order to create a library for the ECCO cell code (part of ERANOS). In order to make sure of the accuracy of the new ECCO library, two benchmark experiments have been analyzed: the MZA and MZB cores of the MOZART program measured at the ZEBRA facility in the UK. These were chosen due to their similarity to the Monju core. Using the JENDL-4.0 ECCO library we have analyzed the criticality of Monju during the restart in 2010. We have obtained good agreement with the measured criticality. Perturbation calculations have been performed between JENDL-3.3 and JENDL-4.0 based models. The isotopes ^{239}Pu, ^{238}U, ^{241}Am and ^{241}Pu account for a major part of observed differences.

Key Words: JENDL-4.0, Fast reactor, Sensitivity and Uncertainty Analysis, ZEBRA Benchmark, Cross-sections processing

1. INTRODUCTION

Before explaining how to process evaluation files in order to make cross-sections libraries for ECCO, it is useful to recall the processing scheme of deterministic codes. The explanations given here are brief. More detailed explanations are available in Ref. [2,3].

Most of the codes used in nuclear engineering are deterministic because they provide accurate results with a short calculation time. All these codes solve an equation – such as the Boltzmann equation or the diffusion equation – in which the unknown is a *function*. As codes use a numerical approach, they cannot handle continuous variables and then have either to discretise the phase space (energy, space, time, angle, etc.) or to decompose the unknown function into a (truncated) series of basic trial functions. The code solves then either a discretized set of equations or the coefficients of the expansion functions. For example, these expansion functions can be Legendre polynomials, spherical harmonics, etc.

There are then different kinds of numerical schemes that can be used : finite differences, finite elements or nodal methods. For a full core calculation with explicit modeling of all core features, the number of unknowns far exceeds the current computers capabilities. This is why intermediate models have to be made and why full core calculations have to be divided into different steps. The most widespread steps are shown in Figure 1 and can be described as follows:

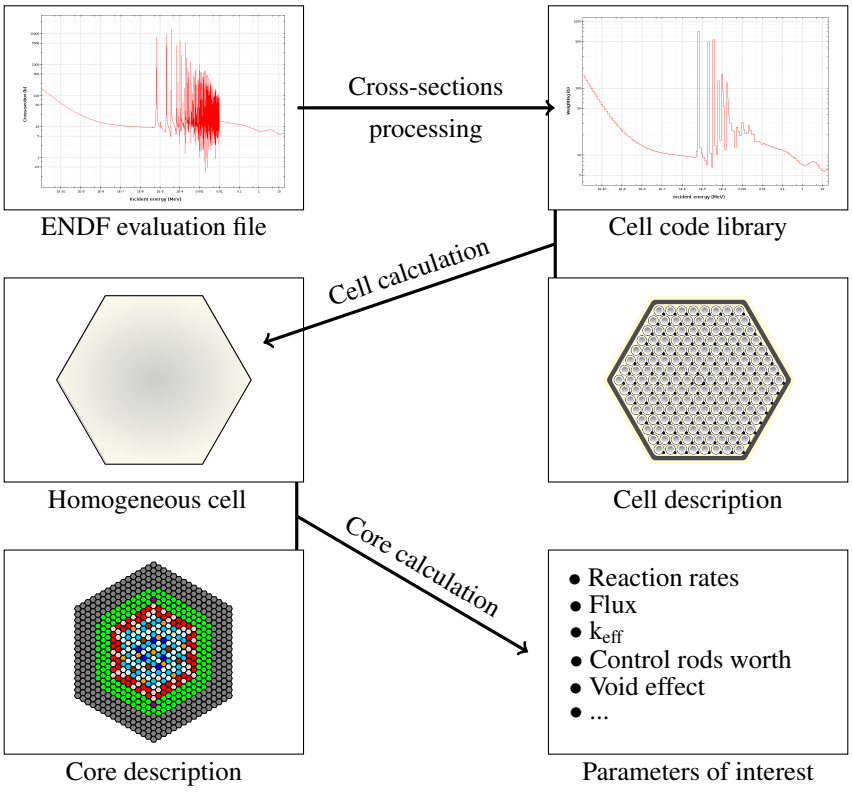

Figure 1. Schematic view of a nuclear reactor calculation

1. The cross-sections processing : Starting from the evaluated data files, reconstruct point-wise cross-sections from nuclear parameters and make multi-group cross-sections. This step is done once for each isotope contained in an evaluation. It provides a cross-sections library, which is specific to the evaluation and that can be used in several situations i.e. for different reactor cores.
2. The cell calculation : The cell calculation consists usually of modeling a representative part of a domain: an assembly with pellets, cladding, coolant, etc. This calculation is usually made in two dimensions. It uses symmetries of the assembly, calculates the flux in the cell, then homogenizes the cell cross-sections over space.
3. The core calculation : The core calculation step uses the homogenized cross-sections from the previous step along with the core loading pattern to calculate the flux using either transport or diffusion theory.

2. CREATION OF A CROSS-SECTIONS LIBRARY FOR ECCO

2.1. Cross-section processing

In the present work, we need to produce a cross-sections library for the cell code ECCO. The process is described in Ref. [4], which provides useful information along with scripts that can be used to process evaluation files. The process is shown in Figure 2 and can be described as follows:

- ENDF formatted files [5] : These are the files made by evaluators considering quantum mechanical models and experimental measurements. They contain data such as evaluated cross-sections but also scattering law data, radioactive decay data and fission yield data, mass, etc.
- NJOY [6] : This processing code reconstructs tabulated point-wise cross-sections. Then it calculates multi-group cross-sections. The process is repeated for several temperatures from 293.6 K to 2973.6 K. NJOY calculates also angular distributions and fission spectra.
- CALENDF [7] : This code calculates several cross-sections and prepares probability tables for specific use in ECCO.
- MERGE is used to merge the output data from NJOY and CALENDF into a single GENDF* file and run tests to check the consistency. By default, cross-sections from NJOY are replaced by CALENDF cross-sections when available. It is possible to manually instruct MERGE to prefer NJOY cross-sections instead of those from CALENDF for certain user-defined energy groups.
- GECCO : This final step adds to the previous GENDF* file some useful data such as mass, disintegration constant or energy reactions. The program also compares the sum of partial cross-sections to the total cross-section and converts the file into the ECCO-library format.

This process has to be done for all JENDL-4.0 isotopes required for Monju modeling. In order to process the ENDF files properly it has been necessary to slightly modify MERGE and CALENDF. At the time of writing, discussions with the experts of CEA are ongoing concerning the processing of several intermediate mass isotopes in CALENDF.

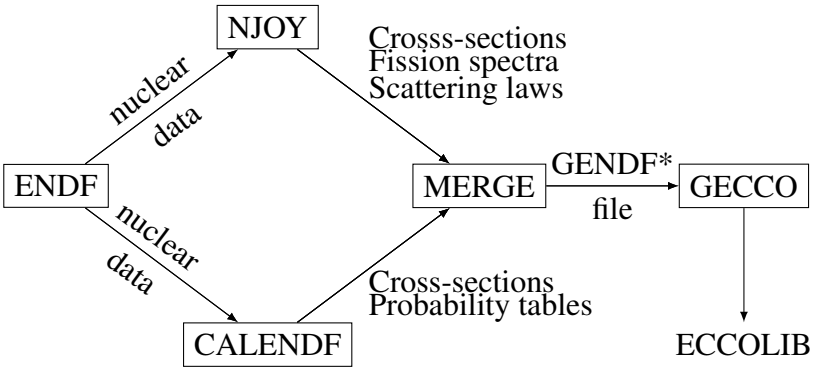

Figure 2. Processing ENDF-6 files into an ECCO library

2.2. Verification of the library processing

To make sure that the processing was correctly done, test calculations were done and comparisons were made with reference libraries. Our institute has three ECCO libraries processed by CEA which have been used as a reference for validation for the following evaluations: JEF-2.2, JEFF-3.1 and JENDL-3.3. Calculations have been done for the infinite multiplication factor (k_∞) for several important isotopes using the CEA "reference" library (*CEA*) and the library that we created (*UF*). The results are shown in Figure 3.

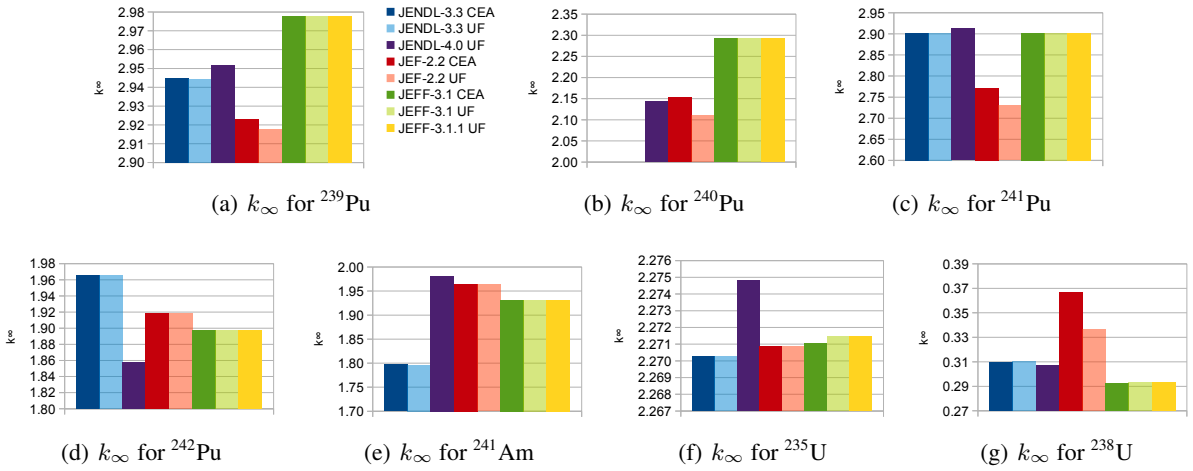

(a) k_∞ for ^{239}Pu (b) k_∞ for ^{240}Pu (c) k_∞ for ^{241}Pu

(d) k_∞ for ^{242}Pu (e) k_∞ for ^{241}Am (f) k_∞ for ^{235}U (g) k_∞ for ^{238}U

Figure 3. k_∞ calculation for several actinides from several evaluations calculated in an infinite medium using ECCO in 1968 energy groups

Large differences are found between the CEA and UF libraries based on JEF-2.2. The difference is assumed to be caused by the use of different subversions of JEF-2.2. Indeed several updates are available for JEF-2.2, and it is not possible to determine which subversion was used for the CEA library. The relevant comparisons are then between JENDL-3.3 and JEFF-3.1 libraries. For those libraries the relative differences of k_∞ between CEA and UF range from 10^{-7} to 4.10^{-4}. Differences

between evaluations are much larger, usually hundreds times larger than differences between the CEA and UF libraries. It was assumed that these results were good enough to consider testing such libraries with core calculations.

2.3. Remaining uncertainties

Nevertheless some features have to be noted. As can be seen in Figure 3(b), ^{240}Pu has not been processed properly for JENDL-3.3, so no k_∞ can be calculated from this isotope. This problem also occurs in the CEA version and was left as is.

^{235}U from JENDL-4.0 (Figure 3(f)) shows a large reactivity *compared* with the other evaluations. This is not an immediate source of concern. In fact, it reported that JENDL-4.0 "improves underestimations for low-enriched uranium systems observed in the JENDL-3.3 results" [8].

Comparison between NJOY and CALENDF cross-sections revealed that for some isotopes and some resonances large differences occur. Such behavior is illustrated in Figure 4 in the case of ^{48}Ti for JENDL-4.0, but this behavior has been observed for several other isotopes as well.

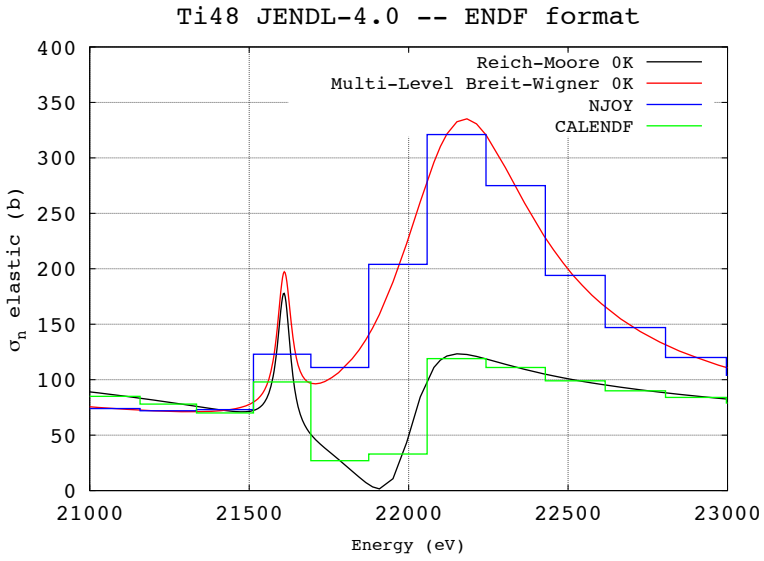

Figure 4. JENDL-4.0, ^{48}Ti: Cross-sections reconstruction with MLBW and RM formalism

This phenomenon seems to be caused by NJOY and CALENDF not interpreting the resonances parameters with the same formalism. The formalism of the resonance parameters is recommended by the evaluators and included in the ENDF file. However CALENDF can chose to use a self-determined formalism in order to be as close as possible to an R-Matrix calculation. Even if this self-determined formalism is expected to be more accurate, it apparently causes a large difference in this case. A comparison with the JANIS data viewer showed that the CALENDF cross-sections for ^{48}Ti in JENDL-4.0 are close to the JEFF-3.1.1 cross-sections of ^{48}Ti in JANIS. At the same time, the NJOY result in Figure 4 for ^{48}Ti in JENDL-4.0 is close to the values cited in JANIS for JENDL-3.3 and ENDF/B-VII. This issue is being discussed with CEA. In some cases, cross-

sections processed by CALENDF are negative. These are replaced by the corresponding NJOY cross-sections. The number of negative cross-sections is small and concern only cross-sections where the corresponding NJOY values are close to zero. Such replacement of CALENDF cross-sections erases the corresponding probability tables. To make sure that this does not have a large effect on a full core calculation, a library was made with only NJOY cross-sections (no probability tables) in 1968 groups. The resulting difference was still small compared with differences between evaluations. It was necessary to enforce CALENDF to use the evaluator formalism for ^{238}U in the JENDL-3.3 evaluation otherwise it triggers cross-section inconsistencies and a high reactivity overestimation.

3. ECCO LIBRARY VALIDATION WITH MZA/MZB

Before applying the JENDL-4.0 ECCO library to Monju analysis it was necessary to estimate its accuracy. The benchmarks selected for the newly made JENDL-4.0 ECCO library are known as ZEBRA-LMFR-EXP-002 in the ICSBEP [9] . This benchmark was elaborated from the ZEBRA-MOZART series of experiments that was held in the ZEBRA Fast Critical Facility at the Atomic Energy Establishment, Winfrith, UK. The program was jointly carried by UKAEA (UK) and PNC (Japan) between 1971 and 1973 and was in support of Monju design. The MOZART program was divided into three phases called MZA, MZB and MZC. The MZA had a simple one-region core and was made for basic physics studies in preparation for the two other cores, which were closer to the neutronic specifications of the Monju design. In the present work, we selected MZA and MZB, which were deemed appropriate for validation of our library.

3.1. Brief core description

There are two major modules in ERANOS to perform flux calculation using transport theory: VARIANT [10] which uses the nodal method in XYZ or Hexagonal-Z geometry and BISTRO [11] which uses the Sn method in RZ geometry. MZA was modeled with both modules to check the consistency between 3D XYZ and 2D RZ modeling. MZB was only modeled in RZ geometry.

Figure 5(a) and 5(c) give a horizontal and vertical view of the MZA core. The assemblies are rectangular steel sheaths in which are stacked different plates. The stacking shows periodicity, the plates of which make a cell motif. A drawing of such a slab cell is shown in Figure 5(d).

3.2. MZA and MZB/3 results using VARIANT XYZ and BISTRO RZ models

The fuel cell calculation was performed in 1968 groups using the dedicated option of ECCO for 2D slab cell description . The reference calculation scheme given in the ECCO documentation [12] involves a 33 group calculation. The 33-group library is obtained from the 1968-group library by collapsing it using an FBR weight flux. Preliminary results showed that 33-group library performance is highly dependent on the weight flux in the fuel region. Thus only the 1968-group library is used for all the fuel cell calculations, which increases considerably the calculation time. Preliminary calculations showed that results based on the 33-group libraries are not consistent (between CEA and UF libraries). For non-fuel cells, sub-critical calculations were nevertheless performed in 33 groups because it was not possible to perform these calculations in 1968 groups. The core calculation for VARIANT is performed using a P3 flux angular development order in 33 energy

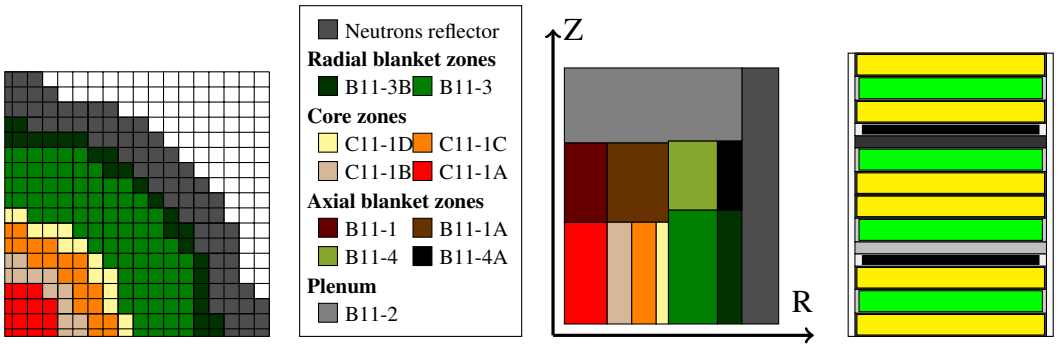

(a) One quarter of MZA core (b) MZA core legend (c) MZA upper half core (d) Scheme of C11-1A cell from MZA

Figure 5. MZA core layout description

groups. The results are similar for a P5 calculation using simplified spherical harmonics. BISTRO was used with the fine *S16_SYMETRIQUE* angular mesh. Some minor isotopes are not present in the 1968 group CEA libraries (JENDL-3.3 and JEFF-3.1) and these have been removed from the both *CEA* and *UF* core models. This impacts lithium, silver, copper, gallium, phosphorus, sulfur and potassium. For JEF-2.2 libraries it also involves ^{238}Pu, ^{234}U, silicon, titanium and molybdenum.

The results of the calculations of MZA and MZB/3 are shown in Table I and II. The RZ model is taken from the benchmark specifications. The Monte Carlo results are also taken from the benchmark documentation [9].

Table I. MZA reactivity calculation

$\frac{k_C-1}{k_C}.10^5$ (k_C)		JEF-2.2	JENDL-3.3	JEFF-3.1	JENDL-4.0
VARIANT	CEA	1343 *(1.01361)*	1571 *(1.01596)*	2174 *(1.02222)*	-
	UF	1758 *(1.01789)*	1693 *(1.01722)*	2201 *(1.02251)*	1907 *(1.01944)*
RZ BISTRO	CEA	1444 *(1.01465)*	1676 *(1.01705)*	2273 *(1.02326)*	-
	UF	1853 *(1.01888)*	1793 *(1.01826)*	2302 *(1.02356)*	1958 *(1.01997)*
Benchmark[a]	MONK	1225 *(1.0124)*	-	-	-
	MCNP	-	922 *(1.00931)*	1373 *(1.01392)*	-
Experimental value (k_E)		960 $\pm$ 160 *(1.0097 $\pm$ 0.0016)*			

[a]For Monte Carlo, the benchmark documentation gives a k_{eff} error of $\pm$ 0.00015.

In this preliminary MZA and MZB calculations, the purpose is to validate the newly made JENDL-4.0 library. So the relevant comparison is more between libraries than with experimental value. UF and CEA libraries give consistent results. Differences between evaluations are larger than between CEA and UF libraries. The difference is large for JENDL-3.3, this appeared to be due to a wrong processing of the ^{238}U-inelastic cross-section in the CEA library. Differences between CEA and UF libraries for JEFF-3.1 can either come from the 33-group processed sub-critical cells, as mentioned

Table II. MZB/3 reactivity calculation

$\frac{k_C-1}{k_C}.10^5$ (k_C)		JEF-2.2	JENDL-3.3	JEFF-3.1	JENDL-4.0
RZ BISTRO	CEA	-512 *(0.99095)*	-271 *(0.99730)*	390 *(1.00391)*	-
	UF	10 *(1.00010)*	-158 *(0.99843)*	416 *(1.00418)*	-135 *(0.998656)*
Benchmark[a]	MONK	685 *(1.0069)*	-	-	-
	MCNP	-	499 *(1.00502)*	878 *(1.00886)*	-
Experimental value (k_E)		438 $\pm$ 100 *(1.0044 $\pm$ 0.0010)*			

[a]For Monte Carlo, the benchmark documentation gives a k_{eff} error of $\pm$0.00015 for MONK and $\pm$0.00012 for MCNP.

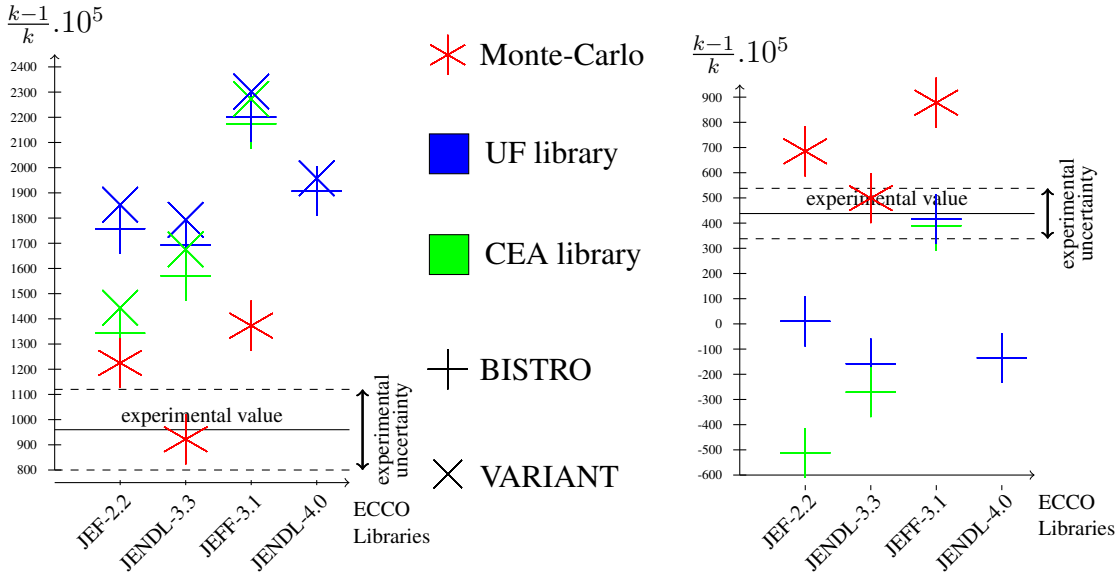

(a) MZA core

(b) MZB/3 core

Figure 6. Reactivity calculation for modeled ZEBRA cores

earlier, or from the library creation process itself.

Comparison with Monte Carlo calculations gives credit to the MZB model even if inherent differences due to Monte-Carlo/deterministic codes remain. The MZA model presents a large overestimation of reactivity, which can be due to lack of anisotropic scattering consideration in the calculation. The core region is small, thus the leakage factor is more prominent than for the larger core MZB. The differences with experimental and Monte Carlo values can also be due to missing isotopes, reducing the internal capture and increasing the reactivity. The MZA XYZ and RZ geometry calculations are consistent, giving credit to the MZB results which are only calculated in RZ-geometry. The newly created JENDL-4.0 library gives each time results that are consistent with other available libraries.

The conclusion of this work was that the JENDL-4.0 based library is adequate to model Monju.

4. MONJU MODELING

4.1. Core description

Collecting data about Monju and modeling its full core required intensive efforts due to strict disclosure rules and scarcity of detailed information related to the core composition. Information given here are from publicly available documentation [13,14,15,16,17]. The modeled core corresponds to the Monju restart core in May 2010. As the experiment was done as a restart, which means zero power test, no temperature profile is required. The core temperature is 180 °C everywhere. Different views of the core are shown in Figures 7(a) and 7(b).

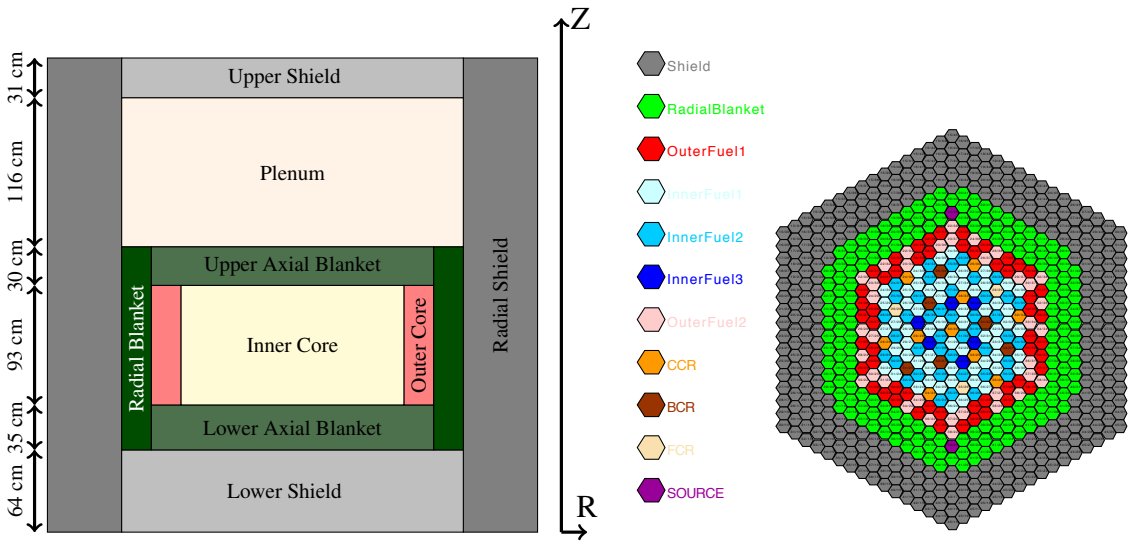

(a) R-Z scheme of Monju core [18]

(b) Loading pattern of Monju [16]

Figure 7. Monju core geometry

4.2. Geometry description

In order to make these descriptions as short as possible, drawings will be used to give the relevant dimensions describing fuel and blanket assemblies. For shield and control rods one is referred to JNC documentation [13]. A fuel assembly description is shown in Figure 8(a); the same geometry applies for all fuel sub-assemblies. The fuel assemblies differ only with their Pu enrichment and composition. All the pins are surrounded with a wire spacer, which has a helical shape around the pin. The wire spacer pitch is 307 mm – this cannot be shown on the 2D figure but it has to be considered for the cell calculation. The blanket geometry is shown in Figure 8(b), in this case the wire spacer pitch is 251 mm.

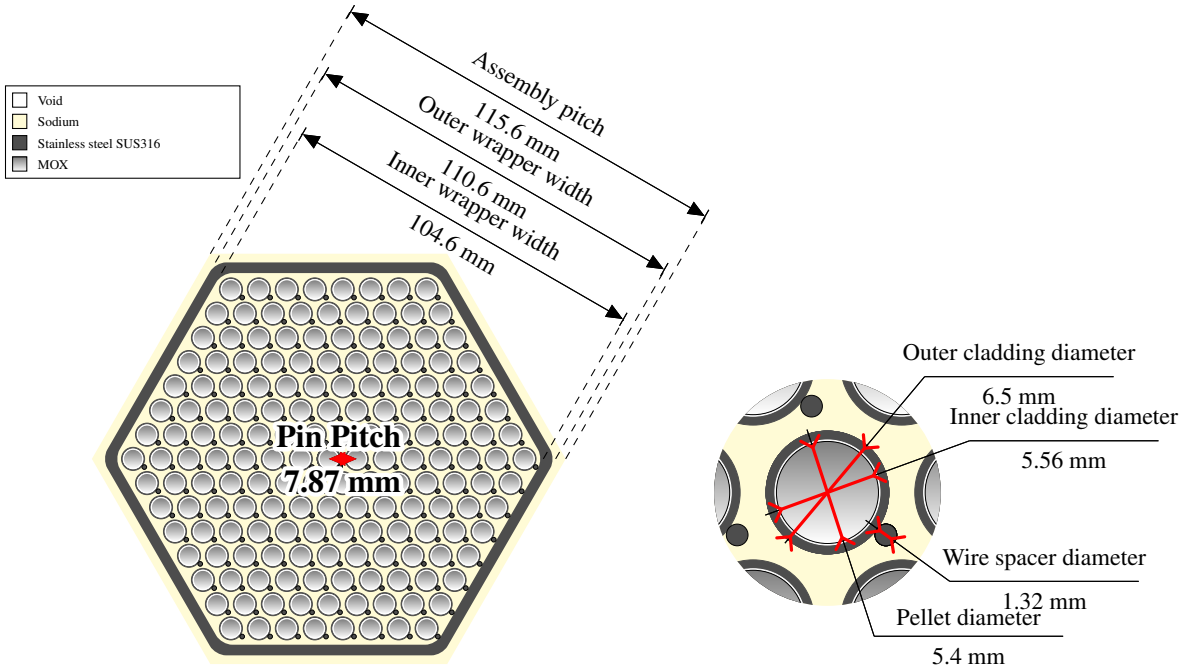

(a) Fuel assembly geometry drawing

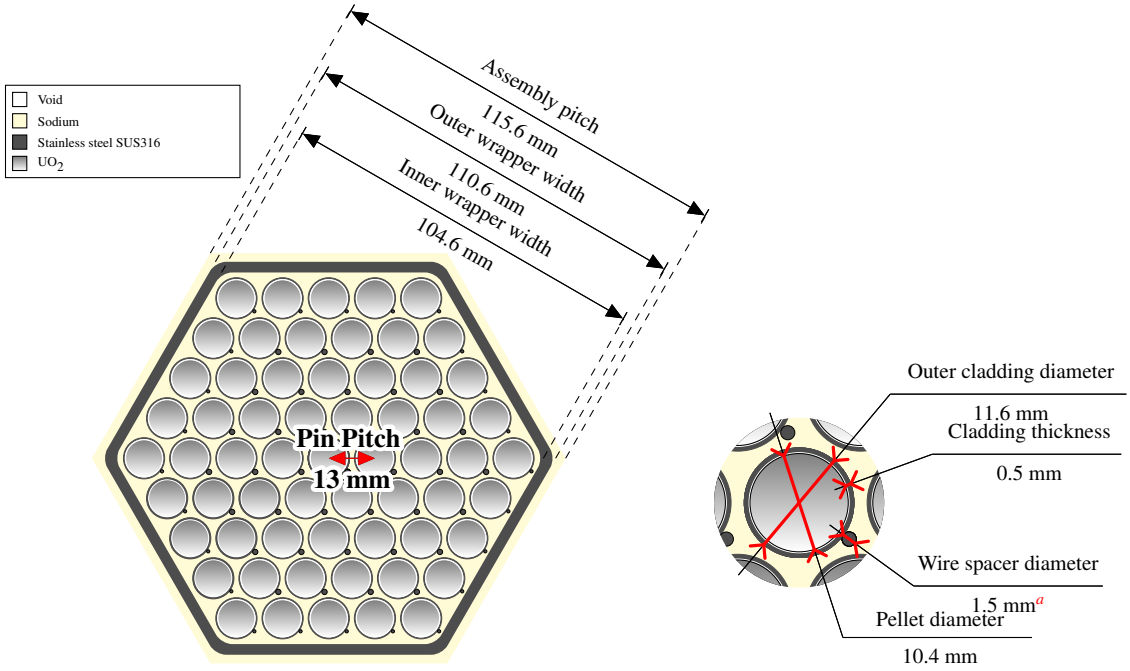

(b) Blanket assembly geometry drawing

Figure 8. Fuel and Blanket assembly of Monju

[a]For the 37 innermost pins the wire spacer diameter is 1.5 mm for the 24 outermost pins it is 0.9 mm. So there is a zoning in blanket assemblies. It has been introduced for thermohydraulic reasons.

4.3. Material compositions

Estimating the fuel composition is not easy. As shown in Figure 7(b), there are five types of fuel assemblies: Inner Core I, II and III and Outer Core I and II. As a starting point, the weight fraction of heavy isotopes for Pu, fissile Pu (^{239}Pu and ^{241}Pu) and ^{241}Am can be found for all fuel types in the NISA report [14]. These values are reported in Table III.

Table III. Plutonium enrichment in wt%, estimation on May 8th 2008

fuel Type	fissile Pu	Pu	^{241}Am	$\frac{\text{Pu+Am}}{\text{M}}$
Inner Core I	13.8	20.0	1.2	21.2
Outer Core I	19.1	27.3	1.4	28.7
Inner Core II	15.3	22.9	1.6	24.5
Outer Core II	20.5	29.5	1.7	31.2
Inner Core III	16.4	24.5	1.1	25.6

Total averaged Pu and ^{241}Am ratio over heavy isotopes can be deduced from Table III and Figure 7(b). They are respectively 24.5wt% and 1.43wt%. This is unfortunately not enough because several isotopic compositions of plutonium can still match with this description. More precise information was eventually found in a JNC document [19], where composition of type Inner I and Outer I are available. The Pu + ^{241}Am isotopic compositions (Pu vector) are reported in Table IV.

Table IV. Isotopic Composition of Fuel I in wt%, estimation on April 6th 1994

Fuel Type	^{238}Pu	^{239}Pu	^{240}Pu	^{241}Pu	^{242}Pu	^{241}Am
Inner Fuel I	1.18	61.58	23.92	7.15	3.95	2.22
Outer Fuel I	1.16	63.02	23.23	7.35	3.76	1.48

Estimations have to be made from type I and transposed to type II and III. Assuming that the fraction of ^{239}Pu – in the Pu-vector – is the same in all the fuel types (62wt%), the fraction of fissile plutonium in the Pu-vector can be deduced from Table III. The fraction of ^{241}Pu can be deduced by subtracting. The fraction of ^{238}Pu and ^{240}Pu have to be assumed to be the same as for the type I (resp. 1.7wt% and 23.6wt%). The content of ^{242}Pu is then deduced by subtracting the overall sum from 100%. The final Pu-vector estimation is available in Table V.

Even if these assumptions lead to the conclusion that type II has been processed slightly before type I, it is the best estimation that can be done with the available documents. As will be presented later, it gives satisfactory results. The uranium enrichment is about 0.2wt% of ^{235}U for all the different fuel types and blanket areas [19].

4.4. Results for VARIANT

The model was then tested with several libraries in order to see if the isotopic composition assumptions were reasonable. It was also a full size test for the processed libraries. These tests were

Table V. Fuel Composition in weight percentage - estimation for May 8th 2008

Fuel Type	^{238}Pu	^{239}Pu	^{240}Pu	^{241}Pu	^{242}Pu	^{241}Am
Inner Fuel I	1.18	61.58	23.92	3.575	3.95	5.795
Outer Fuel I	1.16	63.02	23.23	3.673	3.76	5.157
Inner Fuel II	1.17	62	23.6	0.45	6.25	6.53
Outer Fuel II	1.17	62	23.6	3.71	3.98	5.45
Inner Fuel III	1.17	62	23.6	6.87	4.8	4.3

performed using the VARIANT module of ERANOS. The modeled core correspond to the critical configuration of May 2010 [17]. The results are shown in Figure 9.

As explained for the ZEBRA benchmark, the following results are obtained using 1968 groups cell calculations with ECCO and collapsed into 33 groups for the VARIANT core calculation. Sub-critical areas are directly treated starting from the collapsed 33-group library.

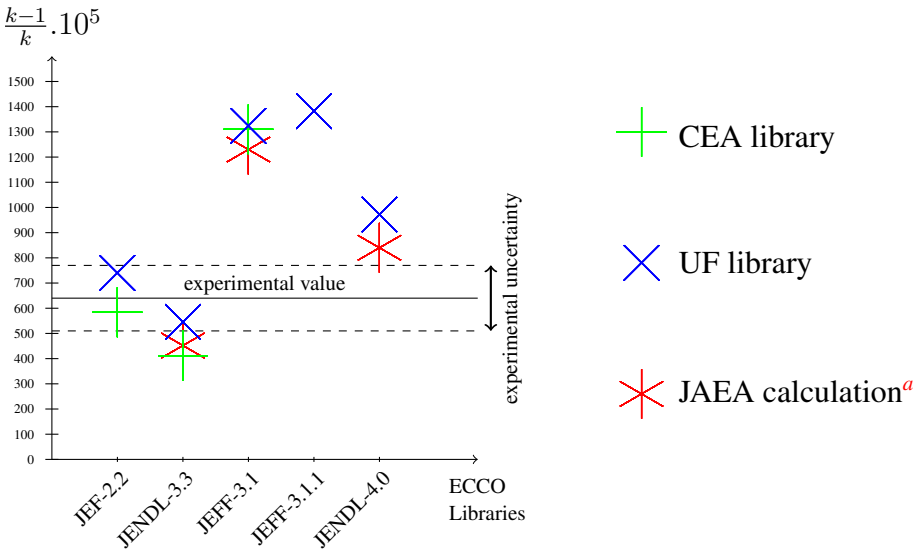

Figure 9. All rods out Monju reactivity

[a]These calculation were made using SLAROM-UF and completely independent codes and libraries [20] but with exact compositions.

In these calculations CEA and UF libraries give small differences: less than 10^{-4}. The remaining differences can not be assumed to come from higher scattering orders; in this test only P1 scattering is used in the ECCO calculations for all libraries. The difference may be due to the numerical processing or due to the sub-critical sub-assemblies being treated using the 33-group collapsed libraries, which has shown less consistency with the CEA ones.

The difference between JAEA and UF calculations are possibly due to more accurate composition definition, burn-up or due to differences in codes; for example, JAEA values are obtained in

70 groups, using diffusion theory with corrections. Differences between UF and CEA libraries remain small and much smaller than differences between evaluations. It is then possible to carry out an analysis of differences between JENDL-3.3 and JENDL-4.0 regarding effects on the Monju reactivity.

5. SENSITIVITY ANALYSIS OF MONJU

In order to use the perturbation/sensitivity analysis modules of ERANOS it is necessary to make an RZ model of Monju because the perturbation module can only treat angular fluxes from BISTRO. The results of this model are shown in Table VI, comparison with nodal 3D calculation is available.

Table VI. Reactivity calculation for Monju restart 2010

$\frac{k_C-1}{k_C}.10^5$ *(k_C)*		RZ SN-BISTRO	HexZ Nodal-VARIANT
JEF-2.2	CEA	336 *(1.00337)*	584 *(1.0059)*
	UF	493 *(1.00495)*	740 *(1.0075)*
JEFF-3.1	CEA	1059 *(1.01070)*	1310 *(1.0133)*
	UF	1074 *(1.01085)*	1326 *(1.0134)*
JENDL-3.3	CEA	155 *(1.00155)*	412 *(1.0041)*
	UF	292 *(1.00293)*	546 *(1.0055)*
JENDL-4.0	UF	718 *(1.00723)*	972 *(1.0098)*
JEFF-3.1.1	UF	1130 *(1.01143)*	1382 *(1.0140)*
Experimental value *(k_E)*		640 $\pm$ 130 *(1.0064 $\pm$ 0.0013)*	

Comparison between RZ and 3D models shows an apparently constant bias between the two models. But as this bias is the same for all the evaluations it is expected to be insignificant in the perturbation calculations.

Once these models are validated, perturbation calculations are implemented in a straightforward manner with the dedicated ERANOS modules. In the perturbation calculations the two considered states are the Monju modeled with both JENDL-3.3 and JENDL-4.0 libraries. In order to get a fine analysis, the *perturbation set* in ERANOS had to be modified in order to decorrelate the σ_f and ν contributions, the results are merged later in a single *sensitivity set*. The results are reported in Figure 10 to 12.

Figure 10 shows the individual contribution of each isotope in the total calculated difference of reactivity. It only represents isotopes that have an actual contribution in the core reactivity change. For example, an isotope for which positive and negative contributions cancel each other is not represented. The red values indicate a negative contribution while the green values indicate a positive contribution to the k_{eff}. Figure 11 shows which reactions (elastic scattering, n,xn, etc.) contribute the most for the most contributing isotopes. Figure 12 shows the detailed energy-structured contribution for the main reactions of the main contributing isotopes.

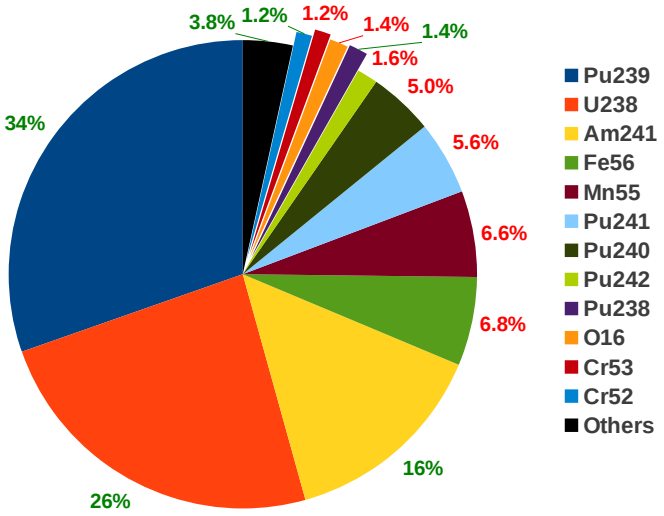

Figure 10. Relative contribution of each isotope to the calculated reactivity difference

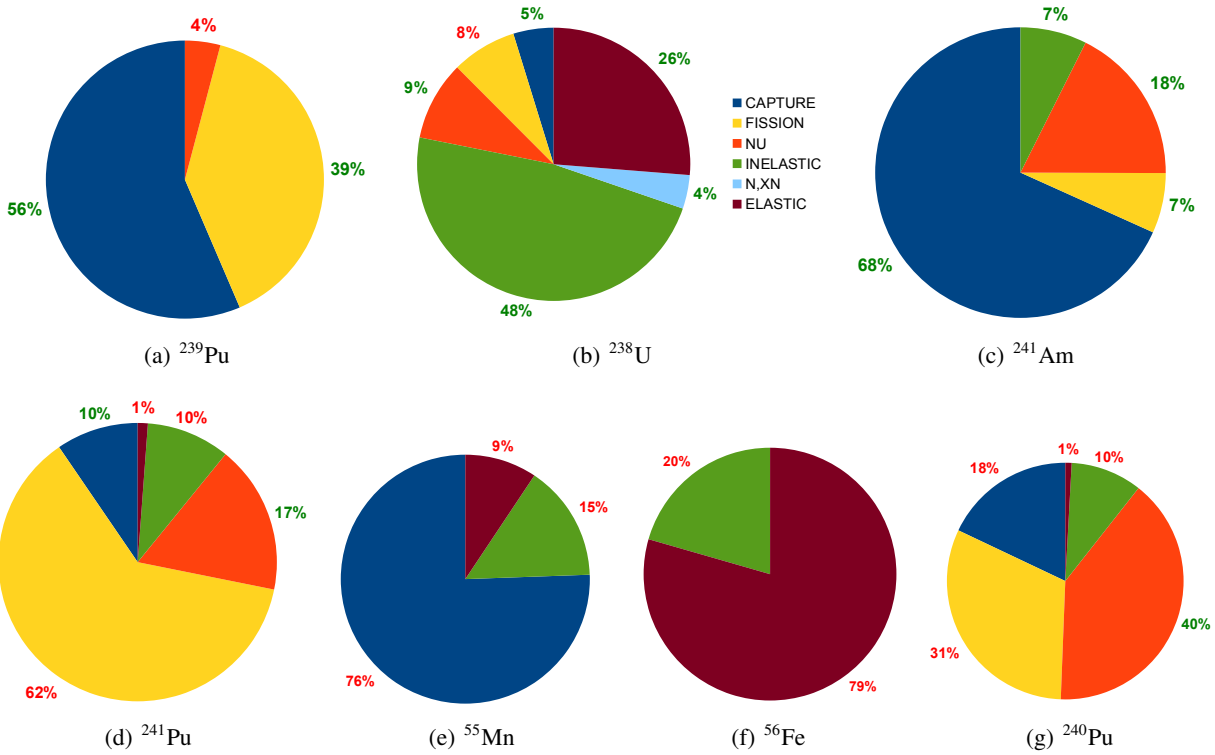

(a) ^{239}Pu (b) ^{238}U (c) ^{241}Am

(d) ^{241}Pu (e) ^{55}Mn (f) ^{56}Fe (g) ^{240}Pu

Figure 11. Breakdown of the contributions of individual reactions for several important isotopes

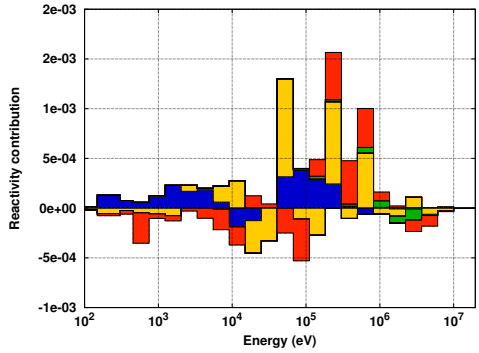

(a) ^{239}Pu

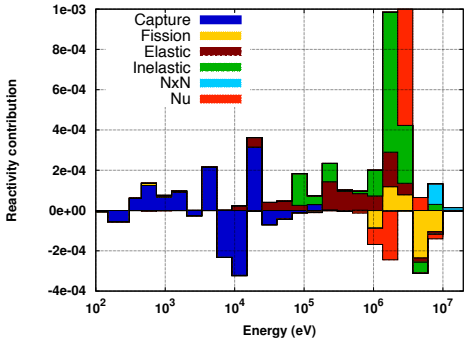

(b) ^{238}U

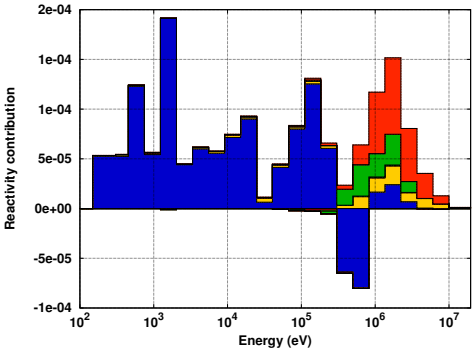

(c) ^{241}Am

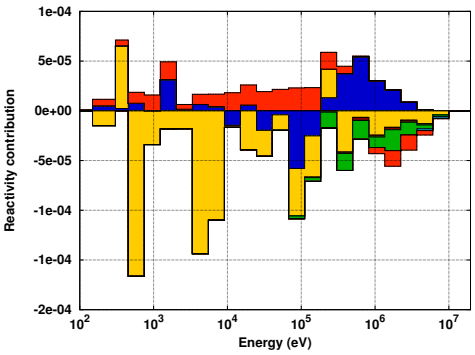

(d) ^{241}Pu

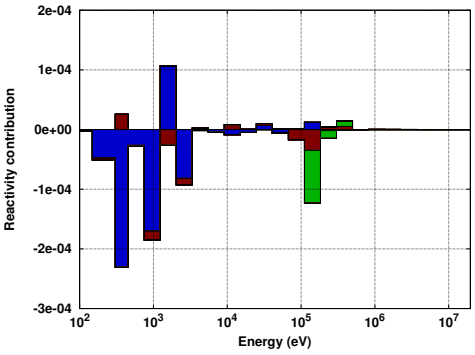

(e) ^{55}Mn

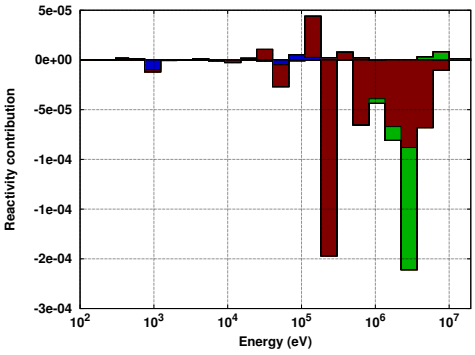

(f) ^{56}Fe

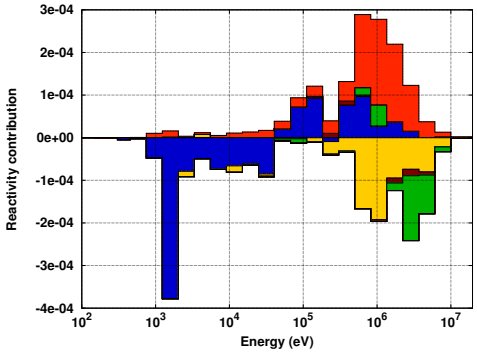

(g) ^{240}Pu

Figure 12. Energy dependency of reactions contribution for the effective isotopes

From these results, the major improvements for Monju reactor in JENDL-4.0 compared with the previous JENDL-3.3 can be summarized as follow:

- Major effective changes are due to actinides.
- ^{241}Am is the third most important isotope even if it accounts for only 1.5% of the reactor content. This is consistent with Ref. [8] where major improvements of ^{241}Am are reported.
- Inelastic scattering in ^{238}U has a major influence even after correction of the ECCO library.
- Capture for ^{239}Pu and ^{241}Am have been effectively updated.
- Fission has been also effectively updated for ^{239}Pu, ^{240}Pu and ^{241}Pu.
- Updates for ν have also an effect for ^{241}Am, ^{240}Pu and ^{241}Pu.
- Unexpected contribution of ^{55}Mn is likely to be due to capture background revaluation by Derrien et al. [21]. Inelastic part is due to CALENDF interpretation of unresolved parameters.

6. CONCLUSIONS

The work presented here resulted in the world's first (to our knowledge) ECCO library based on JENDL-4.0 that can be used for miscellaneous neutronics calculations. The present work also shows the origins of reported improvements brought forward by JENDL-4.0 nuclear set [8]. This work, close to sensitivity calculation, which is a compulsory step for uncertainty analysis. JENDL-4.0 evaluation contains updated covariances matrices, the present work will be used for a future uncertainty analysis of Monju using JENDL-3.3 and JENDL-4.0 in order to confirm these reported improvements.

ACKNOWLEDGEMENTS

The authors would like to thank J.-C. Sublet and O. Bouland (CEA, DEN/DER/SPRC) and P. Ribon (CEA, DEN/DM2S/SERMA) for their help in the ENDF files processing; Japan Atomic Energy Agency for making the internship of Pierre Tamagno possible, and to the European Nuclear Educational Network (ENEN) and Electricité De France (EDF) for their financial support to the study.

REFERENCES

[1] G. Rimpault, D. Plisson, J. Tommasi, R. Jacqmin, J.-M. Rieunier, D. Verrier, and D. Biron. "The ERANOS code and data system for fast reactor neutronic analyses." In *PHYSOR 2002*. ANS, Seoul, South Korea (2002).

[2] P. REUSS. *Précis de neutronique*. EDP SCIENCES (2003). (in French).

[3] W. ROTHENSTEIN and M. SEGEV. *Unit cell calculation*, volume I. CRC Handbook of Nuclear Reactor Calculations (1986).

[4] J.-C. SUBLET, C. DEAN, and D. PLISSON-RIEUNIER. "ECCOLIB-JEFF-3.1 LIBRARIES." Technical Report CEA-R-6100, ISSN 0429-3460, CEA - DEN (2006).

[5] M. HERMAN and A. TRKOV. *ENDF-6 Formats Manual*. Brookhaven National Laboratory, Brookhaven National Laboratory, Upton, NY 11973-5000, USA (2009).

[6] R. E. MacFarlane and D. W. Muir. "The NJOY Nuclear Data Processing System." Technical Report LA-12740-M, Los Alamos National Laboratory, Los Alamos, NM 87544, USA (1994).

[7] J.-C. SUBLET, P. RIBON, and M. COSTE-DELCLAUX. "CALENDF-2005 : USER MANUAL." Technical Report CEA-R-6131, ISSN 0429-3460 (2006).

[8] G. CHIBA, K. OKUMURA, K. SUGINO, Y. NAGAYA, K. YOKOYAMA, T. KUGO, M. ISHIKAWA, and S. OKAJIMA. "JENDL-4.0 Benchmarking for Fission Reactor Applications." *Journal of Nuclear Science and Technology*, **volume 48**, pp. 172–187 (2011).

[9] J. ROWLANDS. *The ZEBRA MOZART Programme Part I. MZA and MZB ZEBRA ASSEMBLIES 11 AND 12* (2008). URL http://www.zebra.webnik.org/Zebra2_Revision1.pdf.

[10] G. PALMIOTTI, C. CARRICO, and E. LEWIS. "Variational Nodal Transport Methods with Anisotropic Scattering." *Nuclear Science and Engineering*, **volume 115**, pp. 233–243 (1993).

[11] G. PALMIOTTI, J. RIEUNIER, C. GHO, and M. SALVATORES. "BISTRO Optimized Two Dimensional Sn Transport Code." In *Topical Meeting on Advances in Reactor Physics, Mathematics and Computation*. Paris, France (1987).

[12] G. RIMPAULT. *PHYSICS DOCUMENTATION OF ERANOS – THE ECCO CELL CODE*. CEA – LEPh (1997).

[13] "Report on nuclear design methods." Technical report, Japan Nuclear Cycle Development Institute (2000). (in Japanese).

[14] "Application for the change of a nuclear reactor facility - JAEA Fast Reactor Development Center - About the nuclear design." Technical Report 111A-2-1, Nuclear and Industrial Safety Agency (2007). (in Japanese).

[15] "Application for the change of a nuclear reactor facility - JAEA Fast Reactor Development Center - Mechanical design of the fuel." Technical Report 111A-1-5, Nuclear and Industrial Safety Agency (2007). (in Japanese).

[16] "Report on the Core Confirmation Tests, submitted to the AESJ Reactor Physics Division." Technical Report 63, JAEA (2011). (in Japanese).

[17] "Core Confirmation Test in System Start-up - Test of the Fast Breeder Reactor Monju." Technical Report 2010-052, JAEA (2011). (in Japanese).

[18] G. TODOROVA, H. NISHI, and J. ISHIBASHI. "Transport Criticality Analysis of FBR MONJU Initial Critical Core in Whole Core Simulation by NSHEX and GMVP." *Journal of Nuclear Science and Technology*, **volume 41**, pp. 493–501 (2004).

[19] "Detailed analysis & evaluation of the core parameters of the Monju FBR." Technical Report 2, Innovative Reactor R&D Company (1995). (in Japanese).

[20] T. HAZAMA (2011). Private communication.

[21] "Original ENDF files."